JOURNAL OF MATERIALS SCIENCE **40** (2005) 2481 – 2485

Effects of CO_2 shielding gas additions and welding speed on GTA weld shape

LU SHANPING, FUJII HIDETOSHI, NOGI KIYOSHI
Joining and Welding Research Institute, Osaka University, 11-1 Mihogaoka, Ibaraki, Osaka 567-0047, Japan

Gas tungsten arc (GTA) welding with deep penetration for high efficiency has long been of concern in industry. Experimental results showed that the small addition of carbon dioxide to the argon shielding gas produces an increase in the weld metal oxygen content, which is one of the compositional variables that strongly influence the Marangoni convection on the pool surface and ultimately change the weld pool shape. An inward Marangoni convection on the weld pool occurs, and hence a narrow and deep weld pool forms when the weld metal oxygen content is over the critical value of 100 ppm. When lower than this value, the weld shape becomes wide and shallow. A heavy oxide layer forms in the periphery area on the pool surface when the CO_2 concentration in the shielding gas is over 0.6%. This continuous heavy oxide layer becomes a barrier for oxygen absorption into the molten pool, and also changes the convection mode on the pool surface. A higher welding speed decreases the heat input and temperature gradient on the pool surface, which weakens the Marangoni convection on the liquid surface.

1. Introduction

Gas tungsten arc welding has been widely used in industry especially for stainless steel, titanium alloys and other nonferrous metals for high quality welds. However, the shallow penetration makes the productivity relatively low. Surface-active elements, such as sulfur, oxygen and selenium of the group VIA, can significantly change the weld penetration in GTA welding when their concentration in the weld pool is over a critical value. Understanding and precisely controlling the effect of surface-active elements on the weld shape are critical for generating a satisfactory weld joint. After decades of development, there are several ways available to add surface-active elements to the weld pool. These active elements can be contained in the material to be welded [1–6], supplied to the welding pool by a pre-placed flux layer on the substrate [7–20] or adjusted by active gaseous addition to the argon shielding gas [21–23]. However, the addition of active elements to substrate sometimes deteriorates its mechanical properties [22]. By smearing a layer of halides or oxides on the plate surface, deep weld penetration was first obtained (ATIG) in the 1960s at the Paton Electric Welding Institute in Ukraine (Kiev) [24]. The flux smearing is not easily applied in automatic welding and it is also difficult for the operator to control the effective quantity of the flux used.

The mixed shielding gas is easily prepared and applied by automatic GTA welding in industry and is therefore desirable if the small addition of the active gas can transfer the surface active element to the weld pool and increase the weld penetration efficiently. However, the investigation of the effect of gaseous additions to the argon-based shielding gas on the weld shape is very limited. From the published literature, Bad'yanov [21], Heiple and Burgardt [22] studied the effect of gaseous fluorides (BF_3, WF_3 and SF_6) and SO_2 additions to the argon shielding gas on the GTA weld shapes and showed that these gases can increase the weld penetration. However, both gaseous fluorides and sulfur dioxide are toxic, which limited their application in industry. Recently, research results showed that the addition of oxygen to the argon shielding gas can significantly change the weld penetration and shape [23].

In this study, the effect of carbon dioxide addition to the argon based shielding gas on the weld pool Marangoni convection and weld shape are investigated using a SUS304 stainless steel substrate in the GTA process. Furthermore, the welding speed effects on the weld pool convection and dimensions are also studied.

2. Experimental

Rectangular SUS304 stainless steel plates ($100 \times 50 \times 10$ mm), with the average composition of 0.06%C, 0.44%Si, 0.96%Mn, 8.19%Ni, 18.22%Cr, 0.027%P, 0.001%S, 0.0038%O and the reminder Fe, were selected as the substrate for the experiments. Prior to welding, the surface of the plate was ground using an 80-grit flexible abrasive paper and then cleaned by acetone.

The CO_2-Ar mixed shielding gas was prepared from pure argon and a premixed argon-0.92%CO_2 or a premixed argon-20%CO_2. For the experiments, the CO_2

content in the shielding gas was in the range of 0.092 to 2%. Direct current, electrode negative (DCEN), automated GTA bead-on-plate welds were made on the center of the prepared plates using a mechanized system in which the test piece was moved at a set speed under the torch. The thoriated tungsten electrode (W-2%ThO_2, Φ1.6 mm) was ground to 60° (vertex angle) before each welding. The electrode gap was set at 3 mm. The welding current was 160A. The mixed shielding gas was supplied at a constant flow rate of 10 L/min. Experiments for different welding speeds from 0.75 to 5.0 mm/s were carried out under Ar-0.1%CO_2 and Ar-0.3%CO_2.

After welding, all the weld beads were sectioned and specimens for the weld shape observations were prepared by etching using a HCl + Cu_2SO_4 solution to reveal the bead shape and dimensions. The cross-sections of the weld bead were photographed using an optical microscope (Olympus HC300 Z/OL). The oxide layer on the weld surface was also observed and photographed. The oxygen content in the weld metal was analyzed using an oxygen/nitrogen analyzer (Horiba, EMGA-520). Samples for the oxygen measurement were cut directly from the weld metal.

3. Results and discussion

3.1. Effect of CO_2 added shielding gas on weld shape

In the GTA welding experiments, the CO_2 concentration in the argon-base shielding gas was changed from 0.092 to 2% at the flow rate of 10 L/min. Representative cross-sections of the welds and the weld depth/width (D/W) ratio for different CO_2 additions are shown in Fig. 1. It is clear that the carbon dioxide added shielding gas had a significant effect on the weld shape. For the low CO_2 addition of less than 0.2%, the weld D/W ratio is low and the weld shape is wide and shallow as shown in area (I) of Fig. 1. When the CO_2 is in the range of 0.2 to 0.6%, the weld D/W ratio is high around 0.5 and the weld shape becomes deep and narrow as shown in area (II) of Fig. 1. With the further increase in CO_2, the weld pool changes to wide and shallow with a concave bottom, which is different from the wide and shallow weld shape with a flat bottom when the CO_2 concentration is below 0.2%.

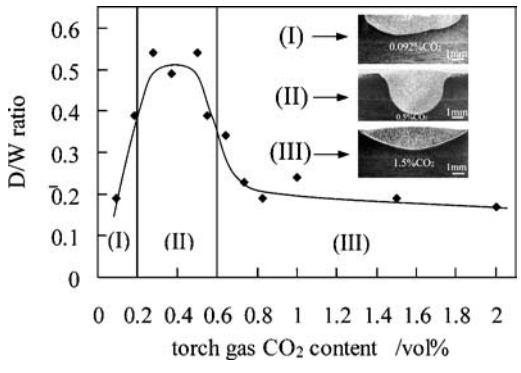

Figure 1 Weld shape and weld depth/width ratio under different CO_2 additions.

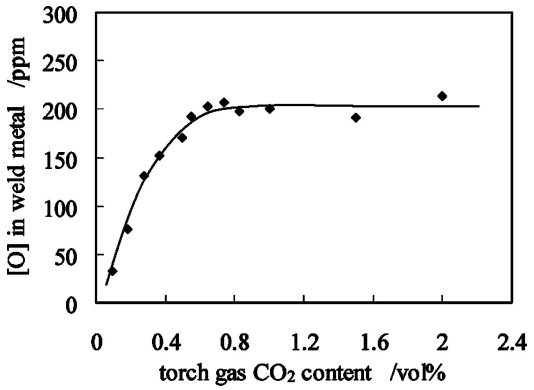

Figure 2 Oxygen content in weld metal under different CO_2 additions.

3.2. Weld metal oxygen content and Marangoni convection

The effect of the torch gas CO_2 concentration on the weld metal oxygen content is shown in Fig. 2. The weld metal oxygen content initially increases with the CO_2 content up to 0.6% and then maintains a nearly constant value around 200 ppm for a CO_2 content up to 2.0%. In the GTA welding process, the weld shape and weld D/W ratio depends to a large extent on the liquid pool convection, which is driven by the surface tension (F_γ), electro-magnetic force (F_{em}), buoyancy force (F_b) and arc plasma drag force (F_P). Among them, the surface tension is one of the main driving forces affecting the liquid pool convection. Heiple and co-workers [5, 12] proposed that surface active elements, such as oxygen, sulfur, selenium and tellurium can change the temperature coefficient of the surface tension for iron alloys. When the surface active element is low in the weld pool, the temperature coefficient of the surface tension is negative, and the Marangoni convection on the pool surface is in an outward direction. Therefore, the heat flux is easily transferred to the edge and the weld shape is wide and shallow. When the surface active elements are high and over a critical value, the temperature coefficient of the surface tension is positive, and the Marangoni convection is inward on the pool surface. In this case, a deep and narrow weld shape forms. Debroy and co-workers [25–27] proposed that the pattern of the Marangoni convection on the pool surface is decided by the combination of the active element content in the weld pool and the temperature distribution on the pool surface. When the peak temperature is high and over a critical value for a weld pool containing a certain active element, such as during stationary GTA welding and laser spot welding, the outward Marangoni convection pattern in the pool center area will coexist with the inward Marangoni convection in periphery area on the pool surface. For this case, the Marangoni convection on the pool surface is complex. However, for the moving GTA welding, this phenomenon seldom happens.

Oxygen from the decomposition of CO_2 provides a significant source of oxygen absorption for the molten weld metal in these experiments. Former research has shown that oxygen is an active element in pure iron and stainless steel in the range of 150–350 ppm [28] and 70–300 ppm [29], respectively. In these ranges, the temperature coefficient of the surface tension of the

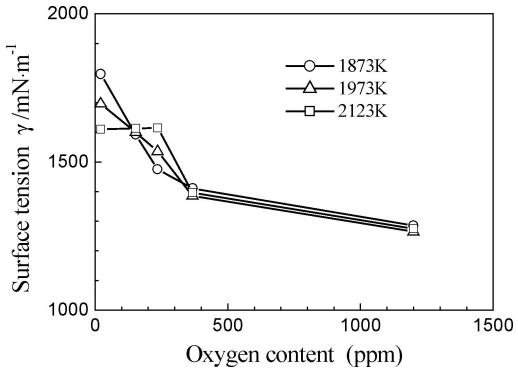

Figure 3 Effect of oxygen content on surface tension of liquid iron.

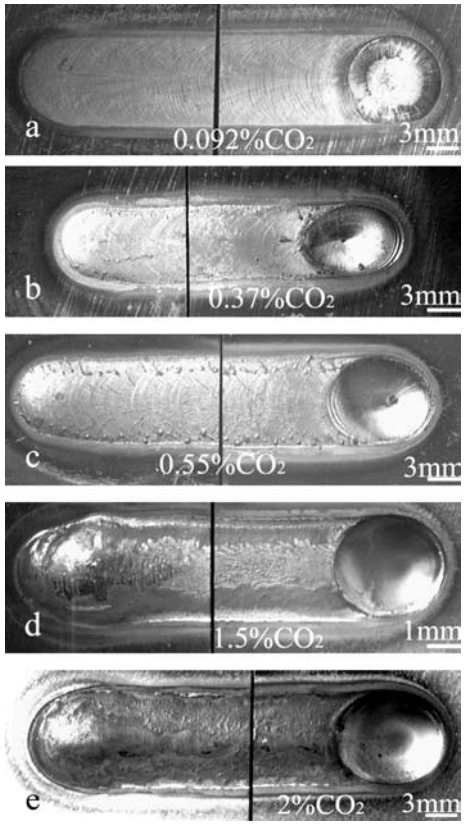

Figure 4 Morphology of oxide layer on bead surface with different CO_2 content in Ar shielding gas of (a) 0.092%, (b) 0.37%, (c) 0.55%, (d) 1.5% and (e) 2.0%.

welding pool is positive, while outside of these ranges, the temperature coefficient of the surface tension becomes negative or nearly zero as shown in Fig. 3 for the Fe-O system. The experimental results from this study are consistent with the former research. When the oxygen content is over 100 ppm in the weld, the Marangoni convection mode is suddenly changed from outward to inward and the shallow-wide weld shape (low D/W ratio) changes to a narrow-deep weld shape (large D/W ratio) as shown in Fig. 1. However, it is interesting to find that the weld D/W ratio decreased suddenly though the oxygen content in the weld is nearly constant at around 200 ppm when the CO_2 addition is between 0.6 and 2.0% as shown in area III of Fig. 1.

3.3. Oxide layer on weld pool surface

The addition of carbon dioxide to the argon shielding gas made the oxidation of the liquid weld pool surface possible. Observations of the surface oxide layer were taken as shown in Fig. 4. When the CO_2 addition in the shielding gas is lower than 0.2%, the weld bead surface is clean and oxides (slag) are invisible to the naked eye as shown in Fig. 4a. When the CO_2 in the shielding gas is increased, there is some discontinuous dotted slag on the two edges of the bead as shown in Figs 4b and c. As the CO_2 concentration is over 0.6% in the shielding gas, a continuous heavy oxide layer is covering the periphery area of the bead surface as shown in Figs 4d and e.

The oxide type and behavior on the liquid pool under the arc column plays an important role in the Marangoni convection of the liquid pool. Thermodynamic calculations of the reactions for the oxides' formation are estimated under the assumption that the weld pool is considered as the Fe-M-O system. The equilibrium reactions of Fe, Si, Cr and Mn with oxygen in the liquid iron were introduced for the oxide products, FeO, SiO_2, Cr_2O_3 and MnO by Kuwana and Sato [30–33]. The equilibrium oxygen content with the iron in the liquid pool based on thermodynamic calculations is listed in Table I under 1773, 1873 and 2273 K. Oxygen analysis of the weld metal showed that the oxygen content in the weld metal is between 30 to 200 ppm as shown in Fig. 2, which is higher than the values of the calculated equilibrium oxygen contents in weld pool for the SiO_2 and Cr_2O_3 oxide formation reactions under the relative lowly temperatures of 1773 and 1873 K as shown in Table I. Therefore, SiO_2 and Cr_2O_3 oxides are possibly formed on liquid pool surface. However, when the temperature is increased to 2273 K, the calculated equilibrium oxygen contents in the liquid pool for the SiO_2 and Cr_2O_3 formation reactions are 0.1922% (1922 ppm) and 0.1495% (1495 ppm), respectively, which is much higher than the experimental values of the weld metal oxygen content. Therefore, the SiO_2 and Cr_2O_3 may not be generated at high temperature. For the moving GTA welding with a weld current of 150 A, and a weld speed of 2.5 mm/s, the peak temperature of the weld pool center is between 2200 and 2500 K for SUS304 stainless steel [26]. In these experiments, the welding current is 160 A and the welding speed is 2.0 mm/s. The peak temperature of the pool should be in the range of 2200 and 2500 K. For this case, the solid Cr_2O_3 (melting point: 2538 K) and SiO_2 (melting point: 2001 K) oxides should form in the periphery area on the weld pool surface, where the temperature is relatively low. In the

TABLE I Equilibrium oxygen content in weld pool by thermodynamic calculations

	Equilibrium oxygen content [%O]		
Oxides	1773 K	1873 K	2273 K
FeO	0.1477	0.2289	0.8985
SiO_2	0.0025	0.0072	0.1922
Cr_2O_3	0.0023	0.0062	0.1495
MnO	0.0263	0.0570	0.5122

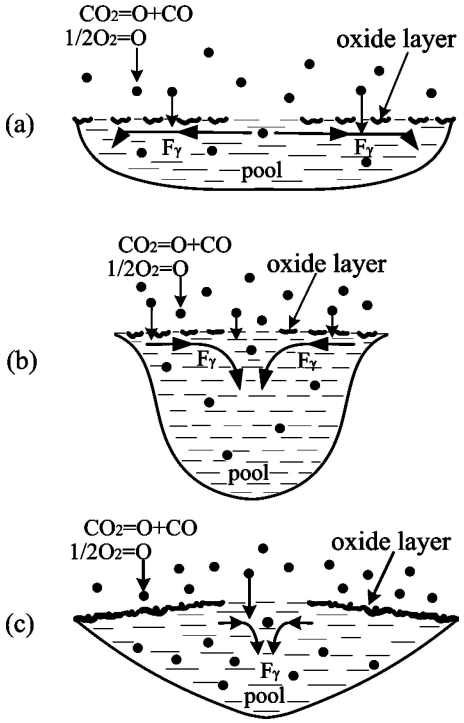

Figure 5 Model for liquid pool convection and oxide layer behavior of (a) quasi-free Pool surface with an outward Marangoni convection for Ar-(0–0.2)%CO_2 shielding, (b) quasi-free pool surface with an inward Marangoni convection for Ar-(0.2–0.6)%CO_2 shielding and (c) restricted pool surface with a heavy continuous oxide layer for Ar-(0.6–2.0)%CO_2 shielding.

liquid pool center area, the temperature is high and the Cr_2O_3 and SiO_2 oxides will not be generated.

One model to illustrate the oxide behavior on the pool surface at elevated temperature is proposed in Fig. 5. When the CO_2 addition is below 0.6%, the oxide layer is thin. This thin oxide layer on the pool periphery area is easily destroyed and exposes the weld pool surface to the arc and shielding gas since the welding pool surface is not stationary and flows under the plasma shear force and surface tension force. Therefore, the oxygen decomposed from CO_2 is easily absorbed and dissolved in the welding pool as shown in Fig. 5a and b. When the CO_2 addition content is below 0.2%, the oxygen in the weld pool is below 100 ppm as shown in Fig. 2. Since the Fe, Ni and Cr have very similar surface tensions and atomic dimensions, and can form nearly ideal solution, the effect of oxygen on the surface tension of the stainless steel can be determined using the data of the Fe-O system as a reference as shown in Fig. 3 [34]. When the oxygen content is below 100 ppm in the Fe-O system, the temperature coefficient of surface tension is negative and the Marangoni convection is outward as shown in Fig. 5a, namely, a quasi-free pool surface with an outward Marangoni convection. Therefore, the weld shape is wide and shallow. When the CO_2 is over 0.2%, the weld metal oxygen content is more than 100 ppm, and the Marangoni convection changes from outward to inward as shown in Fig. 5b, namely, a quasi-free pool surface with an inward convection. In this case, the weld shape is deep and narrow. With a further increase in the CO_2 concentration between 0.6 and 2.0% in the shielding gas, a thick oxide layer forms in the periphery area on the liquid pool surface like Fig. 5c, namely, a restricted pool surface. This continuous thick oxide layer becomes a barrier for oxygen conveyance and absorption into the molten pool. Therefore, the oxygen content in the weld metal remains nearly constant at around 200 ppm as shown in Fig. 2. Because the heavy oxide layer is continuous in the periphery area on the weld pool surface, the liquid pool/oxide layer interface is present instead of the liquid pool/gas surface. In this case, the Marangoni convection due to liquid pool surface tension in the periphery area is no longer the main factor. However, in the pool center area, the inward Marangoni convection still exists because there is no oxide layer on the pool center. This inward convection transports the hot liquid melt at the center of the weld pool from the surface to the bottom. As a result, the weld shape will become wide with a concave bottom as shown in area (III) of Fig. 1.

3.4. Welding speed effect on Marangoni convection and weld shape

The effect of the welding speed was studied from 0.75 to 5.0 mm/s at the constant welding current of 160 A and constant electrode gap of 3 mm. The weld D/W ratio and the weld metal oxygen content are shown in Fig. 6. The weld D/W ratio decreases with the increasing welding speed for the Ar-0.3%CO_2 shielding gas, and remains constant around 0.2 for the Ar-0.1%CO_2 shielding gas. Weld metal oxygen contents are over 130 ppm and around 40 ppm for the Ar-0.3%CO_2 and Ar-0.1%CO_2 shielding gases, respectively. Therefore, an inward Marangoni convection for the Ar-0.3%CO_2 and an outward Marangoni convection for the Ar-0.1%CO_2shielding gas occur during the moving GTA welding process.

The weld shape is dependent to a large extent on the sign and magnitude of the Marangoni convection, which is determined by the temperature coefficient of the surface tension, $\partial\sigma/\partial T$, and the temperature gradient on the weld pool surface, $\partial\sigma/\partial r$. The sign of $\partial\sigma/\partial T$ will determine the Marangoni convection pattern on the surface. The values of $\partial\sigma/\partial T$ and $\partial\sigma/\partial r$ determine the magnitude of the Marangoni convection. Changing the welding speed will alter the heat input per unit length of the weld. A high welding speed will

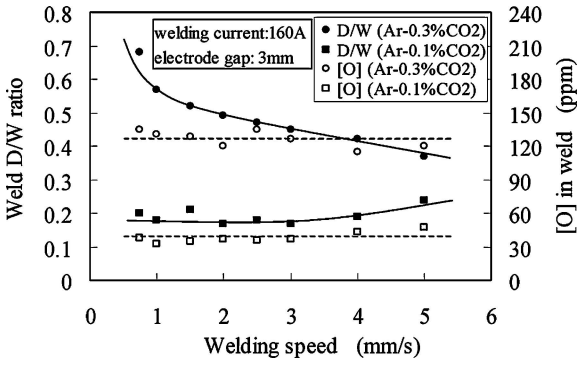

Figure 6 Effect of welding speed on weld D/W ratio and weld oxygen content under Ar-0.3%CO_2 and Ar-0.1%CO_2 shielding gases.

decrease the peak temperature and the temperature gradient on the pool surface. A lower temperature gradient weakens the magnitude of the Marangoni convection on the pool surface, therefore, for the inward Marangoni convection mode under the Ar-0.3%CO_2 shielding gas, the D/W ratio will decrease with the increasing welding speed as shown in Fig. 6. However, for the outward Marangoni convection pattern under the Ar-0.1%CO_2 shielding gas, the weak outward Marangoni convection produces a decreasing weld width with the increasing welding speed, which will impede the decrease in the surface temperature gradient and therefore the weld D/W ratio weakly changes and remains around 0.2.

4. Conclusions

The weld metal oxygen from the decomposition of carbon dioxide in the shielding gas is an active element affecting the Marangoni convection mode on the liquid pool surface during GTA welding process. When the oxygen in the weld is over 100 ppm, the Marangoni convection is inward on the pool surface, and a narrow deep weld shape forms when there is no heavy oxide layer cover on the pool surface. When lower than 100 ppm, it changes to an outward mode and the weld shape becomes wide and shallow

A heavy continuous oxide layer in the periphery area on the liquid pool surface under CO_2-Ar mixed gas shielding protects the liquid pool from being exposed to the shielding gas and becomes a barrier for the oxygen conveyance to the welding pool. In this case, the liquid pool/oxide layer interface is present instead of the liquid pool/gas surface, and the Marangoni convection in the periphery area due to surface tension does not exist again. However, inward Marangoni convection still exists in the pool center area.

Marangoni convection on the weld pool depends to a large extent on the sign and value of the temperature coefficient of the surface tension, $\partial\sigma/\partial T$, and the temperature gradient on the pool surface, $\partial T/\partial r$. An increase in the welding speed will decrease the temperature gradient on the pool surface and weaken the magnitude of the Marangoni convection, which decreases the weld depth/width ratio for inward Marangoni convection.

Acknowledgement

This work is the result of "Development of Highly Efficient and Reliable Welding Technology," which is supported by the New Energy and Industrial Technology Development Organization (NEDO) through the Japan Space Utilization Promotion Center (JSUP) in the program of Ministry of Economy, Trade and Industry (METI), the 21st Century COE Program, ISIJ research promotion grant and JFE 21st Century Foundation.

References

1. H. C. LUGWIG, *Weld. Res. Suppl.* **36** (1957) 335s.
2. B. E. PATON, *Avtom. Svarka.* **6** (1974) 1.
3. W. S. BENNETT and G. S. MILLS, *Weld. J.* **53** (1974) 548s.
4. W. F. SAVAGE, E. F. NIPPES and G. M. GOODWIN, *ibid.* **56** (1977) 126s.
5. C. R. HEIPLE and J. R. ROPER, *ibid.* **60** (1981) 143s.
6. Y. TAKEUCHI, R. TAKAGI and T. SHINODA, *ibid.* **71** (1992) 283s.
7. M. TANAKA, T. SHIMIZU, H. TERASAKI, M. USHIO, F. KOSHI-ISHI and C. L. YANG, *Sci. Tech. Weld. Join.* **5** (2000) 397.
8. P. J. MODENESI, E. R. APOLINARIO and I. M. PEREIRA, *J. Mater. Proc. Tech.* **99** (2000) 260.
9. M. KUO, Z. SUN and D. PAN, *Sci. Tech. Weld. Join.* **6** (2001) 17.
10. D. FAN, R. ZHANG, Y. GU and M. USHIO, *Trans. JWRI.* **30** (2001) 35.
11. D. S. HOWSE and W. LUCAS, *Sci. Tech. Weld. Join.* **5** (2000) 189.
12. C. R. HEIPLE and J. R. ROPER, *Weld. J.* **61** (1982) 97s.
13. P. C. J. ANDERSON and R. WIKTOROWICZ, *Weld. Met. Fabri.* **64** (1996) 108.
14. W. LUCAS and D. HOWSE, *ibid.* **64** (1996) 11.
15. D. D. SCHWEMMER, D. L. OLSON and D. L. WILLIAMSON, *Weld. J.* **58** (1979) 153s.
16. F. LIU, S. LIN, C. YANG and L. WU, *Trans. China Weld. Inst.* **23** (2002) 1.
17. T. PASKELL, C. LUNDIN and H. CASTNER, *Weld. J.* **76** (1997) 57.
18. F. LIU, S. LIN, C. YANG and L. WU, *Trans. China Weld. Inst.* **23** (2002) 5.
19. Y. WANG and H. L. TSAI, *Metall. Mater. Trans.* **32B** (2001) 501.
20. S. P. LU, H. FUJII, H. SUGIYAMA and K. NOGI, *ibid.* **34A** (2003) 1901.
21. N. N. BAD'YANOV, *Avtom. Svarka.* **1** (1975) 75.
22. C. R. HEIPLE and P. BURGARDT, *Weld. J.* **64** (1985) 159s.
23. S. P. LU, H. FUJII, H. SUGIYAMA, M. TANAKA and K. NOGI, *ISIJ. Int.* **43** (2003) 1590.
24. S. M. GUREVICH and V. N. ZAMKOV, *Avtom. Syarka.* **12** (1966) 13.
25. A. PAUL and T. DEBROY, *Metall Trans.* **19B** (1988) 851.
26. T. ZACHARIA, S. A. DAVID, J. M. VITEK and T. DEBROY, *Weld J.* **68** (1989) 499s.
27. *Idem.*, *ibid.* **68** (1989) 510s.
28. H. TAIMATSU, K. NOGI and K. OGINO, *J. High. Temp. Soc.* **18** (1992) 14.
29. S. P. LU, H. FUJII, H. SUGIYAMA, M. TANAKA and K. NOGI, *Mater. Trans.* **43** (2002) 2926.
30. T. KUWANA and Y. SATO, *Trans. Japan Weld. Soc.* **17** (1986) 124.
31. *Idem.*, *ibid.* **7** (1989) 43.
32. *Idem.*, *ibid.* **7** (1989) 49.
33. Y. SATO and T. KUWANA, *ISIJ Int.* **35** (1995) 1162.
34. M. J. MCNALLAN and T. DEBROY, *Metall. Trans.* **22B** (1991) 557.

Received 31 March
and accepted 18 July 2004